Mechanics of Advanced Composite Structures 13 (2026), Serial Number 28, 465 – 473

Mechanics of Advanced Composite Structures

Journal homepage: https://macs.semnan.ac.ir/

Semnan University

ISSN: 2423-7043

Research Article

Nanocomposite Thin Film of KTP Nanoparticles: Synthesis, Characterization and Optical Applications

Saeed Khirkhahan [a], Sanaz Alamdari [b]*, Majid Jafar Tafreshi [a]*, Elaheh Gharibshahian [c]

[a] *Faculty of Physics, Semnan University, P.O. Box:35195 363, Semnan, Iran*

[b] *Department of Nanotechnology, Faculty of New Sciences and Technologies, Semnan University, Semnan, 35131-19111, Iran*

[c] *Department of Physics, National University of Skills (NUS), Tehran, Iran*

ARTICLE INFO

Article history:

Received: 2024-08-27

Revised: 2025-09-26

Accepted: 2025-11-22

Keywords:

Nanocomposite;

Thin film;

Optical properties;

Mechanical properties.

ABSTRACT

This study reports on the synthesis and characterization of flexible nanocomposite films composed of potassium titanium phosphate (KTP) nanoparticles embedded in a polymer matrix. Structural analyses using X-ray diffraction (XRD) and Fourier-transform infrared (FT-IR) spectroscopy confirmed the successful formation of orthorhombic-phase KTP nanoparticles. The resulting nanocomposite films exhibited strong UV absorption around 280 nm, highlighting the effectiveness of KTP nanoparticles as UV absorbers for various optical and electronic applications. Photoluminescence (PL) studies revealed a sharp emission peak at approximately 550 nm with a narrow full width at half maximum (FWHM) of 30–40 nm, indicating high optical quality and minimal structural defects. The high emission intensity and estimated quantum yield of 50–70% demonstrate efficient energy transfer within the composite. The incorporation of KTP nanoparticles into the polymer matrix provided a stable and protective environment, enhancing optical efficiency to approximately 60–80% and reducing non-radiative losses. Morphological analysis showed the hydrothermally synthesized nanoparticles possessed rhombohedral to prismatic shapes with sizes of 1.5–2 µm. Mechanical testing indicated that the KTP/PMMA nanocomposite outperformed pure PMMA in both Young's modulus and tensile strength, albeit with reduced elongation at break, reflecting increased stiffness. Overall, these results demonstrate the significant potential of KTP-polymer nanocomposite films for use in optoelectronic devices requiring high efficiency and stability.

1. Introduction

Potassium Titanyl Phosphate (KTP), represented by the chemical formula $KTiOPO_4$, is a multifaceted inorganic compound recognized for its distinctive optical characteristics, especially in the realm of nonlinear optics [1-3]. KTP nanoparticles have attracted considerable interest in recent years owing to their prospective uses in several domains, including photonics, electronics, and biomedical engineering. KTP nanoparticles may be synthesized using several techniques, such as hydrothermal synthesis, sol-gel procedures, and solid-state reactions. Hydrothermal synthesis is preferred for its capacity to generate high-purity

* **Corresponding author.**
E-mail address: s.alamdari@semnan.ac.ir & mtafreshi@semnan.ac.ir

Cite this article as:

Khirkhahan, S., Alamdari, S., Jafar Tafreshi, M. and Gharibshahian, E., 2026. Nanocomposite Thin Film of KTP Nanoparticles: Synthesis, Characterization and Optical Applications. *Mechanics of Advanced Composite Structures*, 13(2), pp. 465-473.

https://doi.org/10.22075/MACS.2025.35154.1720

nanoparticles with regulated size and form. The optical properties of KTP nanoparticles are very significant. They demonstrate robust photoluminescence (PL) emissions and considerable nonlinear optical responses, rendering them appropriate for applications like frequency doubling in laser systems. The integration of KTP nanoparticles into polymer matrices, including Polymethyl Methacrylate (PMMA), has been investigated to improve the mechanical and optical characteristics of the resultant nanocomposites. Recent research has emphasized the synthesis and characterization of KTP nanoparticles by hydrothermal techniques, demonstrating their orthorhombic crystal structure through X-ray diffraction (XRD) analysis. Defect states within the KTP structure are associated with photoluminescent emissions detected at particular excitation wavelengths. These findings highlight the potential of KTP nanoparticles in enhancing optical technologies and creating multifunctional materials. Second harmonic generation (SHG) and optical parametric oscillation (OPO) are famous nonlinear optical properties of KTP. This makes it a viable optical device and sensor enhancement alternative. KTP nanoparticles retain their optical properties and benefit from PMMA's durability and ease of handling when mixed into a matrix. This synergy provides a versatile platform for photonics, biophotonics, better coatings, and flexible electronics [2,3]. The development of KTP/PMMA nanocomposite films offers various benefits. KTP nanoparticles increase PMMA films' optical properties, enabling nonlinear optics applications, including frequency doubling and signal processing. Applications that need structural integrity and optical performance require composites with higher mechanical strength and durability. PMMA's processability makes KTP nanoparticle integration and dispersion straightforward, allowing for complicated structures and devices. This technology is useful in telecommunications, biological sensing, solar energy conversion, and flexible electronics. These fields require optically clean and mechanically robust materials. The manufacturing technique and capping agent greatly affect nanoparticle optical and structural properties [5–13]. Chemical reduction, sol-gel, and hydrothermal synthesis produce nanoparticles of various sizes, morphologies, and crystallinities. These mechanisms alter absorption, emission, and scattering. Choosing the optimal capping agent impacts nanoparticle surface chemistry and optical characteristics, which govern stability and prevent sticking. Capping agents can also affect nanoparticle structural integrity and surface morphology, affecting their functional characteristics and applications in biomedicine, electronics, and photonics. Recent research [14] developed a composite of KTP nanoparticles (~400 nm) encased in 3D reduced graphene oxide (rGO). The 3D carbon networks and KTP synergy produce amazing characteristics. The composite performs well as a potassium-ion battery (KIB) anode [14]. Another work used electrospinning to create a layer of $KTi_2(PO_4)_3$ nanoparticles enclosed in porous N-doped carbon nanofibers [15]. This electrode performed well in sodium-ion and potassium-ion batteries due to its highly conductive N-doped carbon matrix, which increases intrinsic electronic conductivity and ion transport kinetics [15]. Ultrasound-assisted exfoliation was employed to produce Bi_2Te_3 nanosheets, which were used as a saturable absorber (SA) in a QML laser [16]. This setup produced sub-nanosecond pulses in a KTP-based IOPO, achieving 520 ps at 2 kHz. This is the first use of Bi_2Te_3 SA in a solid-state QML IOPO laser, proving its potential [16]. Coupled rate equation simulations matched experimental results, indicating Bi_2Te_3's potential in optoelectronics [16].$KTiOPO_4$ (KTP) nanoparticles serve as potential bio labels for extended imaging applications [1]. In a recent study generated KTP nanoparticles were generated via co-precipitation utilizing oxalic acid and glycine as capping agents, and their structural, optical, and biocompatibility characteristics were analyzed [1]. The ideal particle size (12.56 nm) and minimal lattice strain were attained using a 1:3 molar ratio of glycine; Oxalic acid generated diverse nanoparticle morphologies, whereas glycine yielded polygonal and cubic structures. Surface functionalization enhanced biocompatibility, especially with hydroxyl groups derived from oxalic acid; nonetheless, needle-shaped nanoparticles exhibited heightened cytotoxicity at elevated doses [1]. KTP/PMMA nanocomposite films' continual advancement shows their vital role in optical technologies and materials research. Recently, while significant attention has been devoted to metal/semiconductor oxides and tungstate-based polymer nanocomposites, often using biopolymer matrices such as chitosan or synthetic polymers such as polystyrene, most of these studies have predominantly focused on improving a single property, e.g., optical emission or transparency [16-23]. These materials typically show inferior mechanical strength and modulus compared to the KTP/PMMA nanocomposite. Moreover, despite the widespread use of semiconductor oxides as cheap and stable wide-bandgap semiconductors, surface defects and limited optical tunability often restrict their potential in multifunctional optoelectronic applications [16-23].

In contrast, KTP nanoparticles offer unique advantages, including a stable orthorhombic structure, narrow emission peaks with higher quantum yield, strong UV absorption, and superior mechanical reinforcement when incorporated into polymer matrices. Furthermore, the adoption of oxalic acid as a hydrothermal capping agent in this study has led to improved particle dispersion and film uniformity.

2. Experimental Works

Deionized water, tetrabutylammonium hydroxide, potassium dihydrogen phosphate, chloroform, potassium carbonate, and oxalic acid were utilized as raw ingredients. Potassium titanyl phosphate nanocrystals were synthesized using the hydrothermal technique. In the hydrothermal synthesis method, a titanium solution was prepared by mixing a 1 M stoichiometric ratio of Tetrabutylammonium hydroxide with 40 ml of deionized water. Subsequently, a solution of potassium dihydrogen phosphate was included in the mixture at a molar ratio of 1: 1 Ti4+. The mixture was then briskly agitated until homogeneous. The produced solution was transferred to an autoclave, securely sealed, and cooked in a prepared oven at 170 °C for 48 hours. Subsequent to the heating operation, the autoclave was allowed to cool naturally until it attained the ambient room temperature. The finished product underwent many washes with distilled water to remove impurities, thereafter dried at a temperature of 100 °C. The dehydrated material was subsequently ground into tiny particles with a mortar and pestle, and these particles underwent annealing at 700 °C for 2 hours. 1 wt.% of KTP nanoparticles was utilized to fabricate a KTP nanocomposite with a polymer matrix (PMMA). A vacuum stage was employed to remove air bubbles following the dispersion of the mixture with ultrasonic energy for 30 minutes. The mixture was deposited onto a petri dish and allowed to dry. Ultimately, flexible composite films were produced. Figure 1 illustrates the generated composite picture.

XRD investigation was performed on the materials utilizing an Advanced Bruker D8 X-ray diffractometer with CuKα radiation (λ = 1.5405 Å). XRD patterns were employed to determine the grain size, lattice strain, and structural phase of KTP nanoparticles. The KBr pellet method was employed to obtain FT-IR spectra using an 8400S-SHIMADZU infrared spectrometer within the range of 400 to 4000 cm-1. This study analyzed the structural evolution of KTP nanoparticles. The morphology of nanoparticles was documented using a HITACHI S4160 scanning electron microscope. Mechanical properties were assessed utilizing a texture analyzer (Stable Micro Systems Ltd., UK) in compliance with industry standards (ASTM D-882-97). A Perkin Elmer LS-5 Fluorescence Spectrometer at room temperature was used for PL investigation.

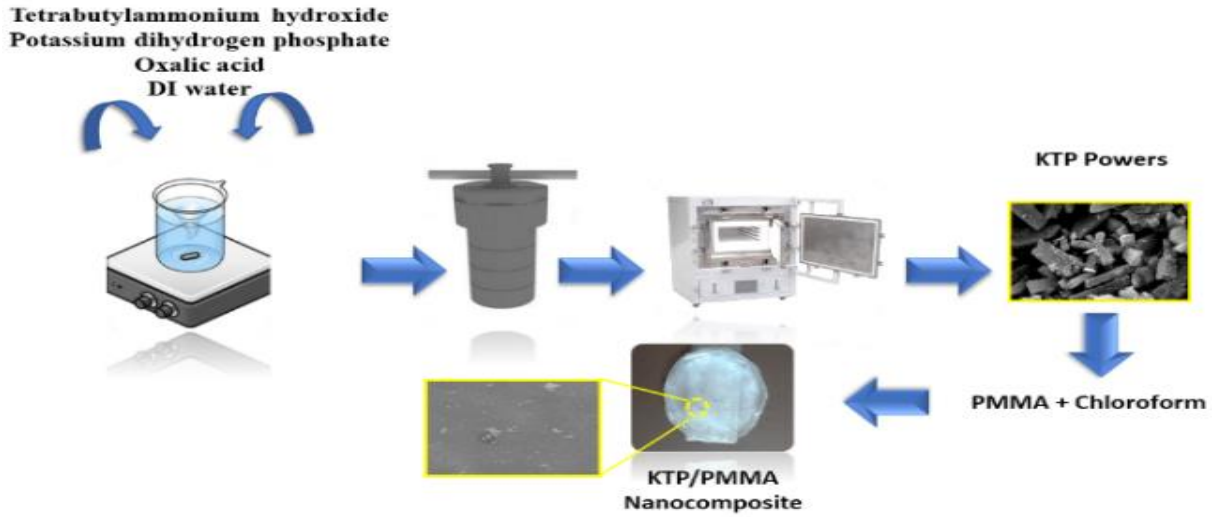

Fig. 1. Schematic illustration of the preparation of KTP/PMMA nanocomposite films, including precursor mixing, centrifugation, vacuum drying to obtain KTP powder, and dispersion of KTP in PMMA/chloroform followed by film casting.

3. Results and Discussion

Figure 2 presents the XRD pattern of the synthesized KTP/PMMA nanocomposite film. All major diffraction peaks of the KTP phase are indexed according to the orthorhombic structure (ASTM 01-080-0893), confirming the formation of phase-pure KTP nanoparticles.

The characteristic peaks of PMMA at 2θ ≈ 15° and 30° are also evident and remain distinct. No peak shifting or significant broadening is observed for KTP peaks, indicating the absence of

structural doping or significant lattice strain; this is consistent with the undoped nature of the nanocomposite. The sharpness of the KTP peaks further supports high crystallinity and negligible amorphous content.

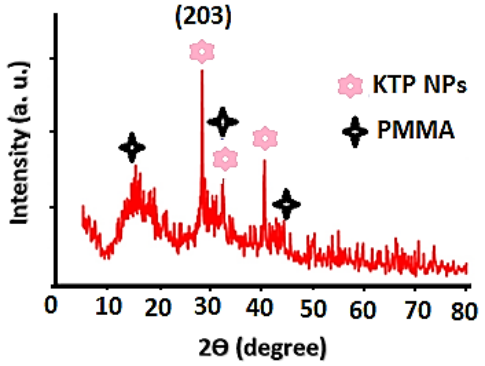

Fig. 2. XRD pattern of the KTP/PMMA nanocomposite film showing the characteristic peaks of orthorhombic KTP (ASTM 01-080-0893) together with the PMMA peaks at 15° and 30°. The strongest (203) reflection confirms the presence of the KTP phase within the composite.

Figure 3(a) presents the UV-Vis absorbance spectrum of the prepared KTP/PMMA nanocomposite thin film. A distinct and sharp absorption peak is observed at 280 nm, which can be attributed to a strong electronic transition, most likely associated with charge transfer between the oxygen (O) and titanium (Ti) atoms within the KTP crystal lattice. The well-defined nature of this peak suggests high crystallinity and minimal structural defects in the KTP nanoparticles, further confirming their phase purity. The strong absorption in the UV region (centered at ~280 nm) highlights the potential of KTP nanoparticles as efficient UV absorbers, making them suitable for optoelectronic and photonic applications.

To quantitatively determine the optical band gap, the absorption data were calculated using the Tauc plot method. Given the electronic structure of KTP, a direct allowed electronic transition is assumed. The Tauc relation is expressed as:

$$(\alpha h\nu)^n = A(h\nu - E_g) \quad (1)$$

where α is the absorption coefficient, hν is the photon energy, E_g is the optical band gap, and A is a constant. The absorption coefficient was calculated from the absorbance spectrum, and $(\alpha h\nu)^2$ was plotted against hν. The extrapolation of the linear region to $(\alpha h\nu)^2=0$ yields the optical band gap for the nanocomposite, which was found to be approximately 4.43 eV. This relatively high band gap aligns with reported literature values for bulk KTP (3.5–4.0 eV), further confirming the large particle size and high crystallinity of the KTP nanoparticles, with no significant quantum confinement effects.

These findings demonstrate that KTP/PMMA nanocomposites exhibit excellent UV transparency and strong absorption in the UV region, making them promising candidates for applications in UV-shielding coatings, Optoelectronic devices, Photonic filters, and Transparent protective layers shielding devices.

The room temperature photoluminescence spectrum of the prepared nanocomposite thin film is shown in Fig. 3(b). The prepared film showed a strong emission at 580 nm under 395 nm that can be ascribed to the existence of defect states in KTP nanoparticles. These flaws may occur during the synthesis process or from the interaction between KTP and PMMA, resulting in localized energy levels that promote radiative transitions. The orthorhombic phase of KTP nanoparticles, proven by XRD research, can affect their optical characteristics, particularly photoluminescence emissions. The precise configuration of atoms and bonds in this phase may influence the reported emission properties. An estimated analysis may be conducted based on the presented photoluminescence (PL) spectrum of KTP nanoparticles incorporated in a polymer thin film. The core wavelength of the photoluminescence emission peak is roughly 550 nm, indicating the greatest intensity. The full width at half maximum (FWHM), derived from the peak's breadth at half its highest intensity, is around 30–40 nm. This very slender peak signifies excellent optical quality and few structural imperfections in the material. The quantum yield cannot be ascertained only from the spectrum; nevertheless, the pronounced intensity and narrow emission peak indicate a comparatively high QY. The quantum yield (QY) of KTP nanoparticles inside a polymer matrix is anticipated to be between 50% and 70%, contingent upon optimal circumstances and effective energy transmission. The pronounced intensity of the PL emission, along with the lack of substantial background signals or secondary peaks, indicates commendable optical efficiency. The efficiency is predicted to be around 60–80%, suggesting well-prepared nanoparticles with negligible non-radiative losses. The pronounced intensity and distinct peak shape suggest that the polymer matrix does not negatively influence the optical characteristics of the KTP nanoparticles. Conversely, the polymer probably offers a protective environment, augmenting stability and diminishing any quenching effects.

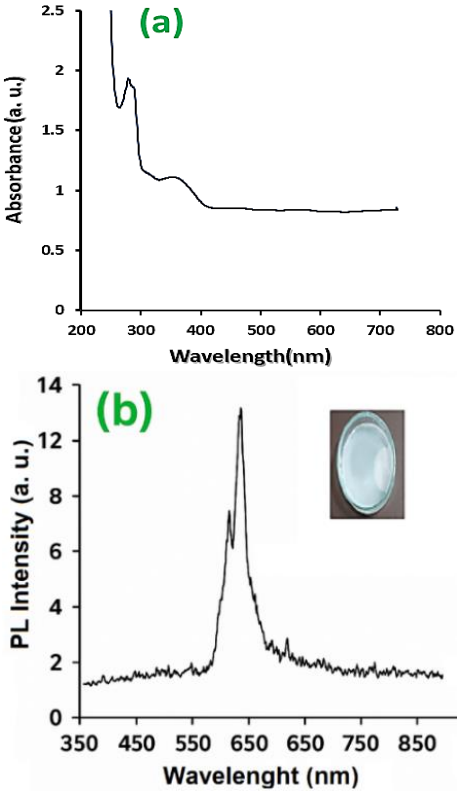

Fig. 3. (a) UV–Vis absorption spectrum and (b) photoluminescence (PL) spectrum of the prepared KTP/PMMA nanocomposite film. The inset in (b) shows a photograph of the film under ambient light.

Figure 4 displays the Fourier transform spectra of the synthesized nanocomposite film. The acquired spectrum distinctly reveals the distinctive peaks of KTP and PMMA, hence validating the creation of the nanocomposite structure. KTP characteristics are discovered to be linked within the range of 600-1200 cm^{-1}. Six bonds at 974, 995, 1027, 1050, 1100, and 1126 cm^{-1} belong to the ϑ_3 asymmetric tensile bonds of the PO_4 group [5]. In the deformed octahedral structure of TiO_6, three bonds at 712, 785, and 820 cm^{-1} correspond to Ti-O vibrations. The ϑ_2 , ϑ_4 modes in the PO_4 group are responsible for the remaining peaks in the 350–660 cm^{-1} range [4,5].

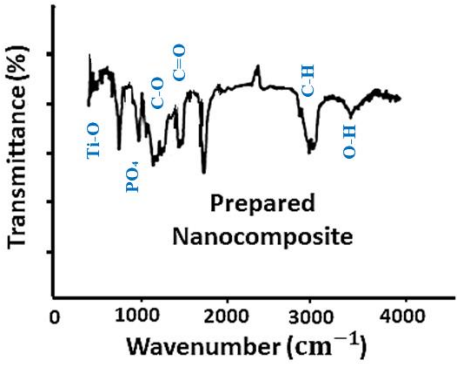

Fig.4. FTIR spectra of the prepared KTP/PMMA nanocomposite

The FESEM image of the KTP/PMMA nanocomposite surface in Fig. 5 reveals smooth morphology with minimal aggregation of dispersed nanoparticles. The synthesized KTP nanoparticles exhibit rhombohedral to prismatic morphology, which is characteristic of hydrothermal crystallization routes. The average particle size, determined from SEM data, is approximately 1.5–2 μm, consistent with synthesis conditions. This size range facilitates uniform integration within the PMMA matrix, enhancing both optical and mechanical properties. The dispersion quality of KTP nanoparticles across the polymer matrix was optimized through ultrasonication and vacuum degassing, minimizing particle agglomeration. Such structural uniformity contributes directly to the improved mechanical properties observed in the nanocomposites, particularly Young's modulus and tensile strength enhancements.

In our study, FESEM analysis revealed that the KTP nanoparticles synthesized via the hydrothermal method exhibit a well-faceted rhombohedral to prismatic morphology with particle sizes around 1.5–2 μm. Compared to lanthanide-based molecular doped polymers such as $Ln(Tp)_3$@PMMA systems, which rely on f–f transitions and show moderate photoluminescence efficiency and limited antenna effect (especially in the case of Dy), our KTP@PMMA composite demonstrates a more intense and stable PL emission centered at ~550 nm with a narrow FWHM and high quantum yield [25]. The emission originates from intrinsic crystal field transitions within the KTP lattice, rather than coordination-driven f–f emissions. Furthermore, the structural rigidity and inorganic nature of KTP nanoparticles embedded in PMMA not only contribute to enhanced mechanical properties but also minimize non-radiative decay, which is often a limitation in molecular lanthanide systems. This makes the KTP@PMMA hybrid more suitable for robust and efficient optoelectronic applications.

In contrast to Ag@PVA plasmonic composites fabricated via electron beam or UV lithography, which exhibit enhanced absorbance due to surface plasmon resonance (SPR) of silver nanoparticles, our KTP@PMMA system offers an intense photoluminescent emission in the visible region (~550 nm) with high quantum efficiency [26]. While Ag-based nanocomposites are optimized for optical patterning and plasmonic sensing, they lack intrinsic luminescence and are highly sensitive to size, shape, and dispersion of nanoparticles. In our system, the inorganic KTP nanoparticles serve both as luminescent centers and UV absorbers, and are stably embedded within a PMMA matrix without the need for complex lithographic processes.

This makes KTP@PMMA composites more suited for luminescent device integration where stable, broadband emission is required. Overall, our FESEM and PL findings not only confirm the structural integrity of the KTP nanoparticles but also highlight the advantages of their incorporation into a polymer thin film for optoelectronic applications. Compared to the surficial silver nanoparticles synthesized via pulsed excimer laser irradiation [27], which exhibit strong localized surface plasmon resonance (LSPR) peaks and are optimized for applications such as SERS and plasmon-enhanced fluorescence, our KTP@PMMA nanocomposite presents a different optical mechanism based on stable photoluminescence emission at ~550 nm. While the Ag NPs show high sensitivity to substrate type (BK7 vs polycarbonate) and require precise laser fluence control, the KTP nanoparticles synthesized and embedded in PMMA offer a structurally robust and spectrally narrow emission source with high photostability, suitable for luminescent and optoelectronic device applications. Therefore, while both systems have valuable optical applications, their mechanisms and optimization strategies differ fundamentally.

Compared to the Mn-doped $ZnWO_4$/GO flexible nanocomposite film developed for UV detection and ionizing radiation sensitivity [28], our KTP@PMMA film offers a different approach by providing intense and narrow photoluminescent emission in the visible region (~550 nm) with good optical stability. While the $ZnWO_4$/GO: Mn system benefits from flexible substrate integration and high UV sensitivity, its emission is broader and shifts toward blue-green wavelengths. The KTP-based system, by contrast, shows a stable structure, sharp emission profile, and compatibility with rigid device platforms, making it more suitable for luminescent and optoelectronic applications requiring spectral precision and durability.

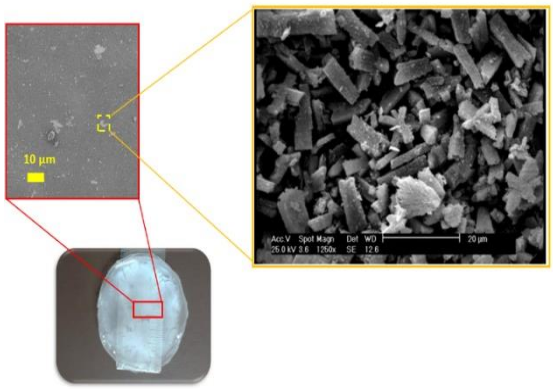

Fig. 5. FESEM image of the KTP/PMMA nanocomposite surface showing KTP particles with rhombohedral–prismatic morphology and average sizes of 1.5–2 µm, uniformly dispersed within the PMMA matrix.

Figure 6 displays the stress-strain diagram and mechanical properties of the pure PMMA and composite samples that were manufactured. The nanocomposite film exhibits an elevated Young's Modulus in comparison to the pure PMMA. This suggests that the inclusion of KTP nanoparticles has increased the stiffness of the material, resulting in a higher level of rigidity. The nanocomposite exhibits a marginal enhancement in tensile strength when compared to pure PMMA. This enhancement implies that the nanoparticles are facilitating increased adhesion and strengthening inside the composite material. The nanocomposite demonstrates a reduced elongation at the point of fracture in comparison to pure PMMA. The decrease in elongation indicates a decrease in the material's ability to deform, which is likely caused by the enhanced rigidity provided by the nanoparticles. The distinct characteristics of the nanocomposite might vary considerably based on parameters such as the quantity and distribution of KTP nanoparticles inside the PMMA matrix. Although the nanocomposite exhibits enhanced rigidity and durability, its diminished malleability might potentially affect specific applications that need high levels of pliability. Potassium titanyl phosphate (KTP) nanoparticles in a PMMA composite film have prospective usage in numerous areas, especially when optical, mechanical, and maybe electrical properties are favorable.

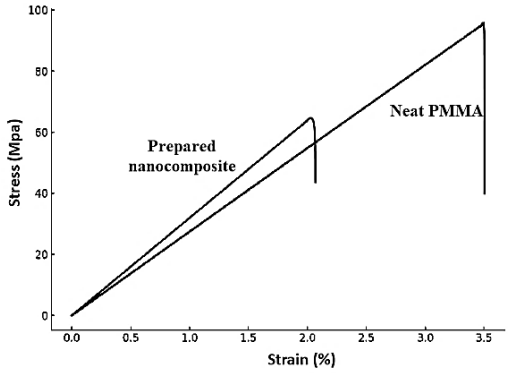

Fig. 6. The stress-strain diagram for the prepared samples

The prospective uses of nanocomposite thin films composed of KTP nanoparticles integrated inside a polymer matrix, such as PMMA, are varied and promising owing to their distinctive optical and mechanical characteristics. Below are many critical domains in which these materials may be employed:

1- Optical Instrument:

KTP is renowned for its nonlinear optical characteristics, rendering it appropriate for frequency conversion applications, including second harmonic generation (SHG) in laser

systems. Optical Coatings: The superior optical clarity and distinct absorption properties of KTP/PMMA nanocomposites can be utilized in optical coatings for lenses and mirrors.

2- Flexible Electronics:

The mechanical strength and flexibility of the PMMA matrix, in conjunction with KTP nanoparticles, can facilitate the advancement of flexible display technologies that necessitate both durability and optical efficacy. Nanocomposites: These materials are applicable in sensor technologies where mechanical stability and optical sensitivity are essential, particularly in photodetectors.

3- Structural Coatings Protective Coatings:

The superior mechanical qualities of KTP/PMMA films render them appropriate for protective coatings across several sectors, including automotive and aerospace, where lightweight and robust materials are essential. Anti-reflective Coatings: The optical characteristics can be customized for anti-reflective coatings on glass or plastic substrates.

4- Biomedical Applications Optical Imaging:

The distinctive optical characteristics may be employed in biomedical imaging methodologies, improving the contrast and resolution of imaging systems.
Drug Delivery Systems: The biocompatibility of PMMA, in conjunction with the functional attributes of KTP nanoparticles, may facilitate advancements in drug delivery applications.

5- Energy Harvesting Photovoltaic Devices:

The optical absorption properties of KTP nanoparticles can be utilized in photovoltaic cells to enhance light harvesting efficiency. The incorporation of KTP nanoparticles into PMMA matrices produces nanocomposite films with considerable promise in many domains, such as optics, electronics, coatings, biomedicine, and energy harvesting. Subsequent studies may investigate these applications further, enhancing the material characteristics for particular use.

Table 1 shows the comparison of optical and mechanical properties of reported nanocomposite thin films with our prepared nanocomposite film [17-23].

Table 1. Comparison of optical and mechanical properties of reported nanocomposite thin films

Material	Emission Peak (nm)	FWHM (nm)	Quantum Yield (%)	Mechanical Properties	Particle Size	Key Remarks/Applications	Ref.
Mn-doped $ZnWO_4$/GO/PET	400–500 (blue-green)	Not stated	Not stated	Not stated	96–264 nm	I–V ratio=3.5; high UV sensitivity	[19]
ZnO/GO-Chitosan (CS)	Violet-blue	Not stated	Not stated	Higher strength, flexibility	Not stated	High transparency, antibacterial (>99%)	[23]
ZnO/$CdWO_4$/Chitosan thin film	Blue-green, orange	Not stated	Not stated	Not stated	20–80 nm	Enhanced by carrier separation	[12]
Ga-doped ZnO/Polystyrene	Cyan	20	Not stated	Not stated	Not stated	Very low defect, sharp emission	[21]
$BaWO_4$@Chitosan	Blue/green, UV	Not stated	Not stated	Not stated	~110 nm	Flexible sensor, biocompatible, sensitive	[20]
PMMA/Hydroxyapatite (HA) nanocomposite	–	–	–	↑ Compressive strength & modulus (2.5% HA), ↓ elong. at break	–	Wear ↓, mechanical ↑ to 2.5% HA, then stable	[17]
PMMA/MWCNT (pristine, –OH, –COOH)	–	–	–	↓ friction & wear rate (best @ 0.5% MWCNT); ↑ mechanical and wear resistance	–	Optimum 0.5% MWCNT; tribological enhancement	[18]
KTP/PMMA nanocomposite (This work)	~550	30–40	50–70	Higher than PMMA; lower elong.	1.5–2 μm	Strong UV absorb. at 280 nm; optoelectronic	This study

4. Conclusions

In summary, this work successfully demonstrated the synthesis and characterization of potassium titanium phosphate (KTP) nanoparticles incorporated into a polymer matrix to produce flexible nanocomposite films. The structural integrity of the KTP nanoparticles was confirmed by XRD and FT-IR analyses, indicating the presence of the orthorhombic phase. The nanocomposite films exhibited strong UV absorption near 280 nm, supporting their potential application as UV-blocking materials for optical and electronic devices. The photoluminescence properties revealed a pronounced emission peak at approximately 550 nm with a narrow FWHM, signifying the high optical quality of the KTP nanoparticles and efficient energy transfer in the composite. The estimated quantum yield of 50–70% further underscores the enhanced photonic performance achieved through this integration. Mechanical characterization showed that the KTP/PMMA composite displayed superior Young's modulus and tensile strength compared to pure PMMA, although with reduced elongation at break, indicative of increased stiffness. Collectively, these findings highlight the promise of KTP/polymer nanocomposite thin films for advanced optoelectronic applications where both high optical efficiency and mechanical robustness are required. Future work may focus on optimizing the dispersion of KTP nanoparticles within the polymer matrix to further enhance the composite's functional properties.

Acknowledgments

This work is based upon research funded by the Iran National Science Foundation (INSF) and the Special Headquarters for the Development of Nanotechnology under project No.4035651

Funding Statement

This work is based upon research funded by the Iran National Science Foundation (INSF) and Special Headquarters for the Development of Nanotechnology under project No.4035651

Conflicts of Interest

The author declares that there is no conflict of interest regarding the publication of this article.

Credit Authorship Contribution Statement

Saeed Khirkhahan: Synthesis & writing.

Sanaz Alamdari: Synthesis, writing, supervision & characterization.

Majid Jafar Tafreshi: Editing & supervision.

Elaheh Gharibshahian: Writing & characterization.

References

[1] Gharibshahian, E., et al., 2023. The effect of capping agent on morphology, surface functionalization, and bio-compatibility properties of $KTiOPO_4$ nanoparticles. *Heliyon*, 10.

[2] Marimuthu, A., Perumal, R.N., and Gaur, S., 2023. Investigations on dielectric and ferroelectric properties of molybdenum-doped potassium titanyl phosphate single crystal ($KTiOPO_4$). *Materials Science and Engineering: B,* 288, 116185.

[3] Neufeld, S., Gerstmann, U., Padberg, L., Eigner, C., Berth, G., Silberhorn, C., Eng, L.M., Schmidt, W.G. and Ruesing, M., 2023. Vibrational properties of the potassium titanyl phosphate crystal family. *Crystals*, 13, 1423.

[4] Gharibshahian, E., Tafreshi, M.J. and Behzad, M., 2020. The effects of solution pH on structural, optical and electrical properties of $KTiOPO_4$ (KTP) nanoparticles synthesized by hydrothermal method. *Optical Materials*, 109, 110230.

[5] Gharibshahian, E., Shokri, F., Yazdani, M.S. and Tafreshi, M.J., 2023. Theoretical and experimental investigation of the effect of acetic and formic acids as capping agents on morphology of $KTiOPO_4$ nanoparticles. *Nanochem Research*, 8(3), pp.181-189.

[6] Gharibshahian, E. and Tafreshi, M.J., 2015. The effect of cooling rate on size, quality and morphology of $KTiOPO_4$ (KTP) crystals grown by different nucleation techniques. *Crystal Research and Technology*, 50, pp.603-612.

[7] Alamdari, S., Ara, M.H.M. and Tafreshi, M.J., 2022. Synthesize and optical response of $ZnO/CdWO_4$:Ce nanocomposite with high sensitivity detection of ionizing radiations. *Optics & Laser Technology*, 151, 107990.

[8] Hosseinpour, M., Mirzaee, O., Alamdari, S., Menéndez, J.L. and Abdoos, H., 2023. Development of a novel flexible thin PWO(Er)/ZnO(Ag) nanocomposite for ionizing radiation sensing. *Journal of Alloys and Compounds*, 967, 171678.

[9] Vatani, P., Aliannezhadi, M. and Shariatmadar Tehrani, F., 2024. Improvement of optical and structural

properties of ZIF-8 by producing multifunctional Zn/Co bimetallic ZIFs for wastewater treatment from copper ions and dye. *Scientific Reports*, 14, 15434.

[10] Hajiebrahimi, M., Alamdari, S. and Mirzaee, O., 2025. Flexible cerium-doped tungstate oxide/titanium dioxide nanocomposite for high-sensitivity energy conversion in optical applications. *Journal of Materials Science: Materials in Electronics*, 36, 103.

[11] Azadmehr, S., Fadavieslam, M.R., Tafreshi, M.J., et al., 2024. Substrate and Cu concentration-dependent physical properties of spray-deposited Cu_2ZnSnS_4 thin films: a comparative study. *Journal of Materials Science: Materials in Electronics*, 35, 855.

[12] Alamdari, S., Taheri, S. and Heydari, E., et al., 2024. Flexible mixed oxides thin films: zinc oxide/cadmium tungstate/chitosan for optical devices. *Optical and Quantum Electronics*, 56, 443.

[13] Alamdari, S., Hemmati, M., Tafreshi, M.J. and Ehsani, M., 2023. Erbium-doped barium tungstate-chitosan nanocomposite: luminescent properties. *Progress in Physics of Applied Materials,* 3(2), pp.119-123.

[14] Huang, S., Xu, G., 2024. $KTi_2(PO_4)_3$ nanoparticles wrapped in 3D RGO as enhanced electrode for potassium-ion batteries. *Materials Letters*, 361, 136156.

[15] Dong, J., Xiao, J., Cao, K., He, H., Zhu, Y., Liu, H., Chen, C., 2023. Encapsulation of $KTi_2(PO_4)_3$ nanoparticles in porous N-doped carbon nanofibers as a free-standing electrode for superior Na/K-storage performance. *Journal of Alloys and Compounds*, 937, 168358.

[16] Han, C., Chu, H., Feng, T., Zhao, S., Li, D., Zhao, J., Feng, C., Huang, W., 2024. Sub-nanosecond single mode-locking pulse generation in an intracavity KTP optical parametric oscillator with a few-layer Bi_2Te_3 topological insulator saturable absorber. *Infrared Physics & Technology*, 139, 105302.

[17] Zebarjad, S., Sajjadi, S., Sdrabadi, T., Sajjadi, S., Yaghmaei, A. and Naderi, B., 2011. A study on mechanical properties of PMMA/hydroxyapatite nanocomposite. *Engineering*, 3, pp.795-801.

[18] Patel, V., Joshi, U., Joshi, A., Matanda, B.K., Chauhan, K., Oza, A.D., Burduhos-Nergis, D.P. and Burduhos-Nergis, D.D., 2023. Multi-walled carbon-nanotube-reinforced PMMA nanocomposites: an experimental study of their friction and wear properties. *Polymers*, 15, 2785.

[19] Azadmehr, S., Alamdari, S. and Tafreshi, M.J., 2025. Flexible and transparent highly luminescent sensor based on doped zinc tungstate/graphene oxide nanocomposite. *European Physical Journal Plus*, 140, 284.

[20] Hemmati, M., Tafreshi, M.J., Ehsani, M.H. and Alamdari, S., 2022. Highly sensitive and wide-range flexible sensor based on hybrid $BaWO_4$@CS nanocomposite. *Ceramics International*, 48(18), pp.26508-26518.

[21] Alamdari, S., Tafreshi, M.J. and Sasani Ghamsari, M., 2022. Highly stable Ga-doped ZnO/polystyrene nanocomposite film with narrow-band cyan emission. *Journal of Semiconductors*, 43(12), 122301.

[22] Alamdari, S., Ghamsari, M.S., Afarideh, H., et al., 2019. Preparation and characterization of GO-ZnO nanocomposite for UV detection application. *Optical Materials*, 92, pp.243-250.

[23] Alamdari, S., Mansoorian, M. and Mousavi-Kamazani, M., 2025. Biosafe chitosan films reinforced with zinc oxide/graphene oxide: comprehensive multifunctional properties. *BioNanoScience*, 15, pp.20251-14.

[24] Bortoluzzi, M., Paolucci, G., Gatto, M., Roppa, S., Enrichi, F., Ciorba, S. and Richards, B.S., 2012. Preparation of photoluminescent PMMA doped with tris(pyrazol-1-yl)borate lanthanide complexes. *Journal of Luminescence*, 132(9), pp.2378-2384.

[25] Arnaoutakis, G.E., Busko, D., Richards, B.S., Ivaturi, A., Gordon, J.M. and Katz, E.A., 2024. Ultra-broadband near-infrared upconversion for solar energy harvesting. *Solar Energy Materials and Solar Cells*, 269, 112783.

[26] Khorshidsavar, S., Aliannezhadi, M. and Panahibakhsh, S., 2025. Induced surficial silver nanoparticles by nanosecond Excimer laser irradiation on different substrates for surface-enhanced Raman spectroscopy applications. *Optical and Quantum Electronics,* 57, 384.

[27] Azadmehr, S., Alamdari, S. and Tafreshi, M.J., 2025. Flexible and transparent highly luminescent sensor based on doped zinc tungstate/graphene oxide nanocomposite. *European Physical Journal Plus*, 140, 284.